Sum Frequency Generation Vibrational Spectroscopy Studies on Protein Adsorption

Jie Wang, Sarah M. Buck, and Zhan Chen*

Department of Chemistry, University of Michigan, Ann Arbor, Michigan 48109

Received: June 6, 2002; In Final Form: August 12, 2002

Sum frequency generation (SFG) vibrational spectroscopy has been successfully applied to detect orientation and conformation changes of adsorbed bovine serum albumin (BSA) molecules at different interfaces. These interfaces include BSA solution/air, BSA solution/fused silica, and BSA solution/deuterated polystyrene (d-PS) interfaces. A general thin film model has been used to interpret BSA SFG spectra. SFG spectra collected from BSA solution/air interfaces with different solution pH are quite different. Detailed analysis indicated that dramatic changes of these spectra are mainly due to the interferences between the C−H signals from interfacial BSA molecules and the O−H signals from water. This has been confirmed by spectra collected from BSA D_2O solution/air interfaces. SFG studies on BSA solution/d-PS interfaces with different solution pH present similar pH dependent results. At BSA solution/fused silica interfaces, only water signals were detected. We believe that the absence of BSA signals was due to the inversion symmetry of hydrophobic side chains buried inside the BSA molecules. Thus, BSA molecules have a "hydrophilic" conformation. Comparison of SFG results at different interfaces shows that C−H signals are greatly varied. Different BSA spectra indicated that BSA structures could be very different while contacting various media. In the literature, research shows that interfacial BSA structures depend on the BSA solution pH. However, our SFG results indicate that these structures still generate similar SFG C−H signals, showing that the alignment and order of C−H functional groups are still similar. Our research of BSA solution/d-PS interfaces demonstrated that SFG can be applied to study protein adsorption on polymer materials in situ.

1. Introduction

Protein adsorption is the first reaction that occurs between a biomaterial and a biological system after it is implanted. Further biomaterial−body interactions, including cell adhesion, inflammation, and blood coagulation, are influenced or controlled by the nature of the initial protein adsorbate. Therefore, whether an implant material will be accepted or rejected by the body (biocompatible or not) is largely determined by protein adsorption.[1−3] Although for decades excellent studies on the interactions between biomaterials and proteins have been performed by many surface-sensitive methods,[4−7] few of which have been in situ molecular level interrogations. Direct in situ information is often difficult to obtain for these interactions because many conventional surface characterization methods require high vacuum.[8,9] Biomaterials, however, are most logically studied in a hydrated environment. In addition, these techniques frequently cannot provide the molecular level information necessary to advance the current understanding of biomaterial interfaces in complex biological milieu. Up to now, no theory of the relationship between implant surface properties and biocompatibility has proven completely satisfactory for improving materials and surface design criteria. The idea that changes in adsorbed protein conformation and composition dictate subsequent biological events is well accepted, but very few molecular level in situ experiments have been performed to prove it.

In recent years, sum frequency generation (SFG) vibrational spectroscopy has become a very powerful and highly versatile spectroscopic tool for surface and interface studies, which not only permits identification of surface molecular species, but also provides information about surface structure, such as coverage and orientation of surface functional groups.[10−22] The SFG technique can be used in ambient conditions to probe any surface or interface accessible by light. It has all the common advantages of optical techniques: it is nondestructive, is highly sensitive, and provides good spatial, temporal, and spectral resolution. In this paper, we demonstrate that SFG can be applied to study structural changes of bovine serum albumin (BSA) molecules adsorbed at different interfaces in situ. We believe that in the future conformational information of adsorbed proteins on a surface, deduced from their SFG spectra, should have correlations with biocompatibility of this surface.

2. Experiment

2.1. Sample Preparation. The BSA solutions (1 mg/mL) studied in this paper were made by dissolving BSA (>99%, fatty acid free, from Sigma) into deionized water. The deionized water (18.2 MΩ-cm) was obtained from a Millipore ultrapure water system. The pH values of protein solutions were adjusted by adding dilute NaOH or HCl aqueous solutions. Deuterated polystyrene (d-PS) was purchased from the Polymer Sources, Inc. and used as received. No C−H signals were detected from the d-PS/air or d-PS/water interfaces, indicating that there were no detectable nondeuterated components. Polymer films were prepared by spin coating. A spin coater from Specialty Coating Systems was used to spin coat 2 wt % polymer/toluene solution at 3000 rpm on fused silica (1" diameter and 1/8" thickness, from ESCO Products) to make polymer films. The polymer films were dried at 80 °C for 12 h.

2.2. SFG Measurements. SFG is a process in which two input beams at frequencies ω_1 and ω_2 mix in a medium and

* To whom all correspondence should be addressed. E-mail: zhanc@umich.edu. Fax: 734-647-4865.

10.1021/jp021363j CCC: $22.00
Published on Web 10/10/2002

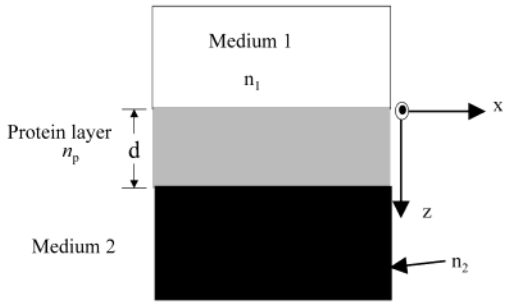

Figure 1. Schematic plot of the adsorbed protein model.

generate an output beam at the sum frequency $\omega = \omega_1 + \omega_2$. Usually, ω_1 is in the visible range, and ω_2 is a tunable infrared beam. If ω_2 is scanned over the vibrational resonances of molecules, the SFG is resonantly enhanced, thus producing a vibrational spectrum characteristic of the material. The intensity of the SFG spectra is related to the average orientation and orientation distribution of functional groups inside the optical field. As a second-order nonlinear optical process, SFG spectral intensity will be zero in a medium with inversion symmetry under the electric-dipole approximation. SFG spectra can be detected from the material where the inversion symmetry is broken. Most bulk materials have inversion symmetry, thus they do not generate SFG signals. We believe that SFG can be applied to study orientation or conformation changes of interfacial protein molecules, where inversion symmetry is broken.

The SFG setup in our lab has been described in detail before.[23−26] Briefly, sum frequency spectra were collected by overlapping a visible and a tunable IR beam on a surface or interface, at incident angles of 60° and 54°, respectively. The visible beam had a wavelength of 532 nm, and was generated by frequency-doubling the fundamental output pulses of 20 ps pulse width from an EKSPLA Nd:YAG laser. The IR beam, tunable from 1000 to 4300 cm^{-1}, was generated from an EKSPLA optical parametric generation/amplification and difference frequency system based on LBO and $AgGaS_2$ crystals. The diameters of both beams on the sample were about 0.5 mm. The sum frequency signal was collected by a photomultiplier tube. In this work, SFG spectra with ssp polarization combination (s-polarized SFG output, s-polarized visible input, and p-polarized infrared input) were collected.

The experimental geometry to collect signals from polymer/protein solution and fused silica/protein solution interfaces was similar to that for collecting spectra from polymer/water interface, which was described previously.[23,26]

3. Results and Discussion

3.1. Model to Treat SFG Spectra from BSA Molecules. We have collected SFG spectra of BSA molecules from the BSA solution/air, BSA solution/fused silica, and BSA solution/d-PS interfaces. Research shows that protein adsorption may not always be a monolayer adsorption. Also, BSA is a large protein (~65 kD) and may behave very differently than the small molecules that SFG is generally used to study. These two factors make it necessary to reevaluate the analysis usually applied to small molecules forming a monolayer. Instead of using a simple interface to interpret the protein SFG spectra, the more general thin film model should be applied.[27] In this paper, the analysis of adsorbed protein layer between two different media was based on this model.

We consider the absorbed protein layer to be a film with a thickness of d between two media (Figure 1); d is assumed to be smaller than the coherent length and wavelengths of the input and output optical fields. The SFG output in terms of energy per pulse from the thin film in the reflected direction can be written as[27]

$$S(\omega) = \frac{8\pi^3\omega^2\sec^2\beta}{c^3 n_1(\omega) n_1(\omega_1) n_1(\omega_2)} |\chi^{(2)}_{\mathrm{eff}}|^2 I_1(\omega_1) I_2(\omega_2) AT \quad (1)$$

where $n_1(\omega_i)$ is the refractive index of the incident medium at frequency ω_i, ω is the frequency, β is the reflection angle of the sum frequency field, $I_1(\omega_1)$ and $I_2(\omega_2)$ are the intensities of the two input fields with frequencies ω_1 and ω_2, T is the pulse-width of both input lasers, and A is the overlapping cross section of the two input beams at the sample. The effective second-order nonlinear susceptibility, $\chi^{(2)}_{\mathrm{eff}}$, of the adsorbed protein layer can be written as [27−30]

$$\chi^{(2)}_{\mathrm{eff}} = [\hat{e}(\omega)\cdot\vec{\vec{L}}(\omega, z=0)]\cdot\vec{\vec{\chi}}^{(2)}_{1\mathrm{p}}:[\hat{e}(\omega_1)\cdot\vec{\vec{L}}(\omega_1, z=0)][\hat{e}(\omega_2)\cdot\vec{\vec{L}}(\omega_2, z=0)] + [\hat{e}(\omega)\cdot\vec{\vec{L}}(\omega, z=d)]\cdot\vec{\vec{\chi}}^{(2)}_{2\mathrm{p}}:[\hat{e}(\omega_1)\cdot\vec{\vec{L}}(\omega_1, z=d)][\hat{e}(\omega_2)\cdot\vec{\vec{L}}(\omega_2, z=d)] + \int_0^d [\hat{e}(\omega)\cdot\vec{\vec{L}}(\omega, z)]\cdot\vec{\vec{\chi}}^{(2)}_{\mathrm{p}}:[\hat{e}(\omega_1)\cdot\vec{\vec{L}}(\omega_1, z)][\hat{e}(\omega_2)\cdot\vec{\vec{L}}(\omega_2, z)]dz \quad (2)$$

where $\vec{\vec{L}}(\omega_i, z)$ is a diagonal tensor. It behaves like a macroscopic local field factor (Fresnel coefficient factor) in relation to the optical field inside the thin layer, which can be calculated by Fresnel law of thin film.[27] The terms $\vec{\vec{\chi}}^{(2)}_{1\mathrm{p}}$, $\vec{\vec{\chi}}^{(2)}_{\mathrm{p}}$, and $\vec{\vec{\chi}}^{(2)}_{2\mathrm{p}}$ are second-order nonlinear susceptibility tensors of the interface between the absorbed proteins and medium 1, the absorbed protein film, and the interface between the absorbed proteins and medium 2, respectively.

Under the electric-dipole approximation, the second-order nonlinear susceptibility tensor $\vec{\vec{\chi}}^{(2)}$ determined in the laboratory frame (x, y, z) can be expressed in terms of the molecular hyperpolarizability tensor $\vec{\vec{\alpha}}^{(2)}$described with respect to the molecular frame (a, b, c):[31−33]

$$\chi^{(2)}_{ijk}(z) = n_p(z) l_{ii}(\omega, z) l_{jj}(\omega_1, z) l_{kk}(\omega_2, z) \sum_{\xi,\eta,\zeta} < (\hat{\imath}\cdot\hat{\xi})(\hat{\jmath}\cdot\hat{\eta})(\hat{k}\cdot\hat{\zeta}) > a^{(2)}_{\xi\eta\zeta} \quad (3)$$

Here $\chi^{(2)}_{ijk}$ is an element of tensor $\vec{\vec{\chi}}^{(2)}$. The resulting expressions carry the orientation and orientation distribution information of functional groups obtainable from SFG measurements. The term $n_{\mathrm{p}}(z)$ is the density of the functional group. It also may vary across the film. The angular brackets denote an average over the molecular orientational distribution. The tensor $\vec{\vec{l}}(\omega_i, z)$ describes the microscopic local field correction which can be evaluated by Lorentz model.[31,34] For a simple condition where the refractive indices of the two media and the absorbed protein layer are very similar, the Fresnel coefficient factor and the local field correction factor can be considered constant, and eqs 2 and 3 will have the same form as the simple interface model:[35]

$$\chi^{(2)}_{\mathrm{eff}} = [\hat{e}(\omega)\cdot\vec{\vec{L}}(\omega)]\cdot\vec{\vec{\chi}}^{(2)}:[\hat{e}(\omega_1)\cdot\vec{\vec{L}}(\omega_1)][\hat{e}(\omega_2)\cdot\vec{\vec{L}}(\omega_2)] \quad (4)$$

$$\chi^{(2)}_{ijk} = N_{\mathrm{s}} l_{ii}(\omega) l_{jj}(\omega_1) l_{kk}(\omega_2) \sum_{\xi,\eta,\zeta} < (\hat{\imath}\cdot\hat{\xi})(\hat{\jmath}\cdot\hat{\eta})(\hat{k}\cdot\hat{\zeta}) > a^{(2)}_{\xi\eta\zeta} \quad (5)$$

where $N_{\mathrm{s}} = \int_0^d n(z)\, dz$.

Under this condition, functional groups with random distribution or with inversion symmetry in the film will not generate SFG signal under the dipole approximation. If SFG signals from

any functional group are observed, then this functional group is not randomly orientated and must have some order or favored orientation. We can use the SFG signal detected from various functional groups to deduce the favorable orientations of each group in the absorbed protein layer. If we can determine the average orientation and orientation distribution of all functional groups in the adsorbed protein molecules, we can possibly understand detailed conformational changes of absorbed proteins at different interfaces. The denaturation of proteins at interfaces can be detected by comparing their interfacial structures to native proteins.

Real situations may be much more complicated than assumed above. The assumption that the Fresnel coefficients and local field correction factors do not vary across the protein layer may not be valid. Under such conditions, even functional groups that have a distribution with inversion symmetry may generate SFG signals. Therefore, in order to interpret SFG spectra correctly, evaluating the local field change across the film is necessary. If we assume that functional groups inside the film are distributed with inversion symmetry, and thus their SFG signal is only due to the variation of the optical field across the film, we are able to evaluate whether the changes in the optical field have a significant effect on the interfacial protein signal. Because of the complexity of the integration and accurate determination of refractive indices inside the film, we apply an approximation to evaluate the Fresnel factors and local field corrections contributed to the SFG signals generated from these groups. In this approximation, we separate all of the functional groups inside the film into two parts. Each of the two parts has the local field of the upper or the lower contacting medium, respective to its position in the film. Then, the eq 2 becomes

$$\chi^{(2)}_{\text{eff}} = [\hat{e}(\omega)\cdot\vec{\vec{L}}(\omega,z=0)]\cdot\vec{\vec{\chi}}'^{(2)}_{1p}:[\hat{e}(\omega_1)\cdot\vec{\vec{L}}(\omega_1,z=0)][\hat{e}(\omega_2)\cdot\vec{\vec{L}}(\omega_2,z=0)] + [\hat{e}(\omega)\cdot\vec{\vec{L}}(\omega,z=d)]\cdot\vec{\vec{\chi}}'^{(2)}_{2p}:[\hat{e}(\omega_1)\cdot\vec{\vec{L}}(\omega_1,z=d)][\hat{e}(\omega_2)\cdot\vec{\vec{L}}(\omega_2,z=d)] \quad (6)$$

$\vec{\vec{\chi}}'^{(2)}_{1p}$ and $\vec{\vec{\chi}}'^{(2)}_{2p}$ are second order nonlinear susceptibility tensors of the two parts. Under this approximation, these two parts have the same group density and orientation distribution with opposite orientation direction. SFG intensity calculated from this approximation will provide us with a basic idea of how strong SFG signals can be generated by local field changes inside the film of functional groups that have a distribution of inversion symmetry. In our experiments, measured SFG signal intensity from the protein solution/air interface is about one magnitude larger than the result calculated above. These strong signals observed cannot be solely due to the local field effect. The interfacial protein molecules must have orientation or conformation changes induced by different interfaces.

Various second-order nonlinear susceptibility components can be obtained by fitting SFG spectra using:[24]

$$I \propto |\chi^{(2)}_{\text{NR}} + \sum_q \frac{A_{\text{eff},q}}{\omega_2 - \omega_q + i\Gamma_q}|^2 = |\chi^{(2)}_{\text{NR}} + \sum_{q_1}^{\text{Group1}} \frac{A_{\text{eff},q1}}{\omega_2 - \omega_{q1} + i\Gamma_{q1}} + \sum_{q_2}^{\text{Group2}} \frac{A_{\text{eff},q2}}{\omega_2 - \omega_{q2} + i\Gamma_{q2}} + \cdots|^2 \quad (7)$$

where $A_{\text{eff},q}$ is related to the appropriate $\vec{\vec{\chi}}^{(2)}$ tensor elements through the Fresnel factors and $\chi^{(2)}_{\text{NR}}$ is the nonresonant background.

3.2. BSA at Different Interfaces. SFG has been applied to investigate orientation and conformation of BSA molecules adsorbed at different interfaces, including BSA solution/air, BSA solution/fused silica, and BSA solution/d-PS interfaces. Deuteration of PS ensures that all C−H signals collected from BSA solution/polymer interfaces are due to BSA molecules. After we prepared the interfaces, we waited for at least 30 min and then started to collect SFG spectra.

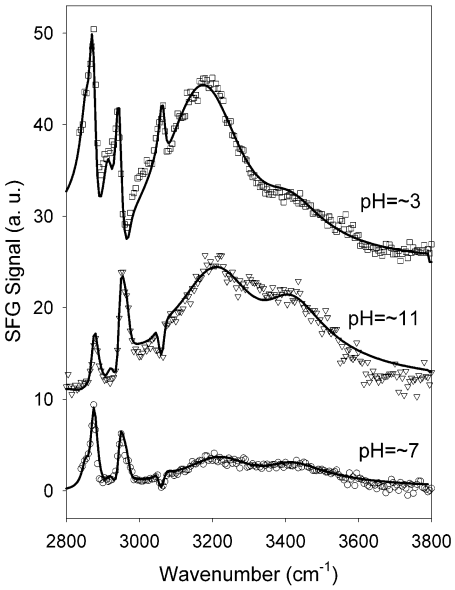

Figure 2. SFG spectra of BSA solution/air interfaces with different solution pH values.

3.2.1. BSA Solution/Air Interface. The BSA solution/air interface has been investigated by different research groups using various techniques.[36−41] All of the experiments indicate that BSA is surface active and tends to segregate to the surface. However, the detailed structural information of adsorbed BSA molecules at the solution/air interface has not been reported yet.

The SFG spectra of BSA solution/air interfaces at different solution pH are shown in Figure 2. We believe that these SFG signals of BSA molecules come mainly from the absorbed BSA layer at the surface. The SFG intensity from any particular aligned functional group (with the same orientation) is proportional to the square of the concentration of this group. Because the concentration of BSA molecules outside this adsorbed layer in solution decreases dramatically,[4] and are randomly oriented, the contribution of BSA molecules in solution to the SFG signal should be insignificant. This can be confirmed experimentally by collecting SFG spectra from the BSA solution/air interface while varying the concentration of BSA solution. The intensities of SFG spectra collected from the BSA solution/air interface with concentrations of BSA solution ranging from 0.05 to 1 mg/mL show no substantial change. If the signal from the BSA solution dominates the SFG spectra, the intensity should be very sensitive to the concentration of the solution.

From Figure 2, it is clear that features of all three SFG spectra of BSA solution/air interfaces with different solution pH values of ~3, ~7, and ~11 are different. The aliphatic C−H stretches from 2800 to 3000 cm^{-1}, aromatic C−H stretches around 3060 cm^{-1}, and O−H stretches at higher wavenumbers are all markedly different. The question now becomes whether different spectral features in Figure 2 show that BSA molecules have distinctly different structures at solution/air interfaces with different solution pH values. It is well-known that varying pH can induce secondary structural changes of BSA molecules in solutions.[42] To accurately compare the interfacial structures of BSA molecules at solution/air interfaces with BSA solutions

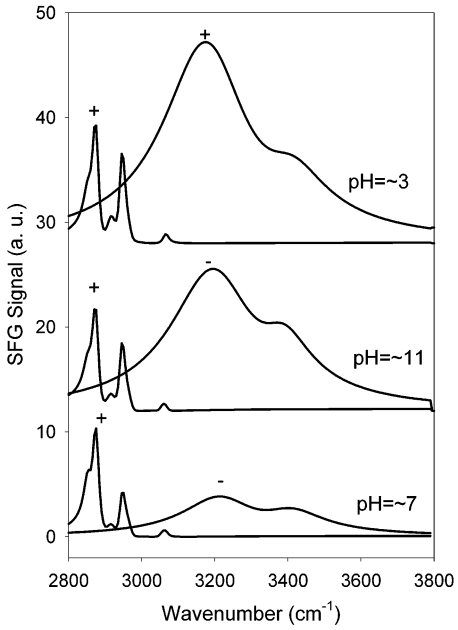

Figure 3. Fitting results for Figure 2.

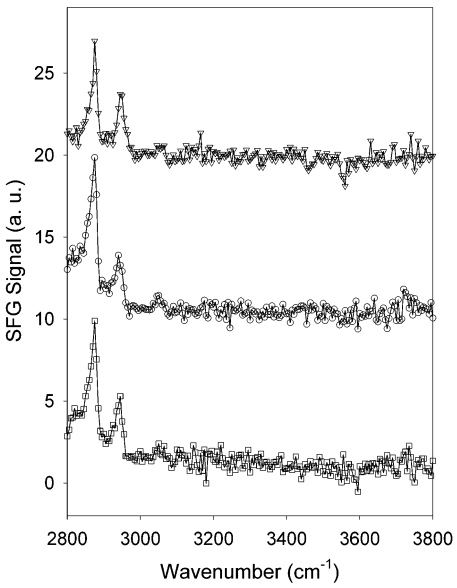

Figure 4. SFG spectra of BSA D_2O solution/air interfaces with different solution pH values. Starting from the top spectrum, pH values are 3, 11, and 7.

of different pH values, fitting the SFG spectra in Figure 2 quantitatively is necessary.

The fitted SFG spectra by using eq 7 are displayed as lines in Figure 2. The calculated fit approximates the experimental data quite well (shown as dots). For a more clear demonstration, the contributing factors in the spectra are displayed separately as C−H signals and O−H signals in Figure 3. Clearly, the spectral features for the C−H stretches collected from solutions of different pH are quite similar; but the spectral features in the O−H stretching region are different. The relative phases between C−H and O−H signals are quite different in different spectra; this causes the very different overall spectral features of SFG spectra in Figure 2. According to the fitting results shown in Figure 3, there are four different interfacial functional groups which contribute to the SFG spectra: methylene, methyl, phenyl, and hydroxyl groups. The peaks around 2855 and 2920 cm^{-1} are assigned to the symmetric and asymmetric stretches of methylene groups, the peaks at 2875, 2940, and 2965 cm^{-1} are due to the stretching modes of methyl groups, the peak around 3060 cm^{-1} is from the phenyl groups, and broad peaks around 3200 and 3400 cm^{-1} are from O−H stretches. According to the molecular structure of BSA,[43−47] SFG signals of normal methyl groups are contributed from side chains of amino acids valine, leucine, isoleucine, threonine, and alanine. The aromatic C−H signal of phenyl groups can only come from three amino acids: phenylalanine, tyrosine, and tryptophan. We believe that O−H signals are mainly contributed from interfacial water molecules. There are only three amino acids that have hydroxyl groups: threonine, serine, and tryptophan. BSA only has a small amount of these three amino acids.

To confirm our conclusion that major differences of three spectra depicted in Figure 2 are due to different phases between C−H and O−H signals rather than different C−H and O−H stretches themselves, we collected SFG spectra of BSA D_2O solution/air interfaces with different solution pH (Figure 4). O−D stretches of water molecules shift to lower wavenumbers (∼2300−2600 cm^{-1}) and would not interfere as strongly as O−H stretches with C−H signals from BSA molecules. SFG spectra of C−H modes at different pH in Figure 4 are similar. They are also similar to the fitted spectra shown in Figure 3. The spectral features of O−D signals at lower wavenumbers (not shown) are similar to the fitted O−H contribution to the SFG spectrum of the BSA H_2O solution/air interface with the same solution pH.

The phase differences between C−H and O−H signals at different solution pH are due to opposite relative orientations between methyl or phenyl groups of BSA molecules and water molecules at the interface. The hydrophobicity of a functional group largely determines the orientation as measured by SFG. It is well know that the hydrophobic head of surfactants will point to air at water surface. Similar to the surfactants, we believe that methyl and phenyl groups of BSA molecules at the solution/air interface tend to point to the air. The water molecules at the interface have varying orientations because the surface BSA have different charges at different pH levels. For solutions with pH below the isoelectric point (p$I \approx 4.8$), BSA molecules carry a net positive charge. Likewise, above the isoelectric point, the proteins carry a net negative charge. The change in charge of the protein molecule induces a change in water alignment near the protein layer in accordance with water's dipole moment. This alignment is responsible for the 180° phase change of the water O−H stretches one sees between the pH 3 and 11 spectra. Regardless of the alignment, the water O−H signal interferes with the C−H signal of the protein; whether that interference is constructive or destructive is dependent on the relative phases of the stretching signals. This is the main effect responsible for the differences in spectra at various pH levels.

According to the neutron reflection studies, the adsorbed BSA at the solution/air interface is nearly a monolayer. The surface concentration of BSA is ∼3 mg/m^2 or $\sim 2.7 \times 10^{12}$ molecules/cm^2 (deduced from the protein volume).[36] Comparing the SFG intensity of the symmetric stretches of methyl groups to that of known standard, such as z-cut quartz,[48,49] the absolute intensity of methyl groups from absorbed protein layer at pH around 7 is equal to one layer of methyl groups perpendicular to the water surface with a surface density of $\sim 1.0 \times 10^{14}$ /cm^2. BSA has only about 300 methyl groups per protein molecule,[50] so this high estimation of methyl coverage is surprising. We confirmed this measurement by comparing the SFG intensity of methyl symmetric stretch of BSA solution/air interface to that of poly(*n*-butyl-methacrylate) (PBMA)/air interface. PBMA has a high

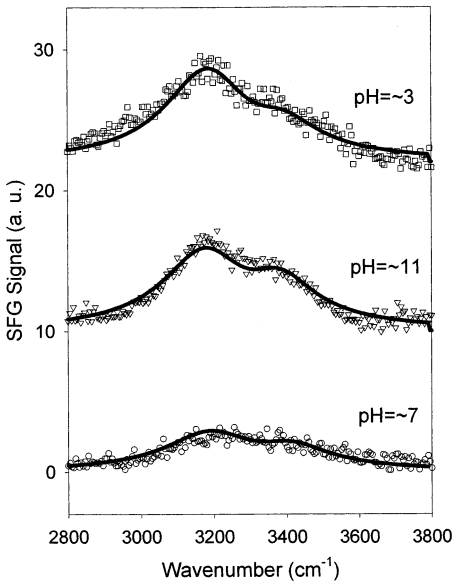

Figure 5. SFG spectra of fused silica/BSA solution interfaces with different solution pH values.

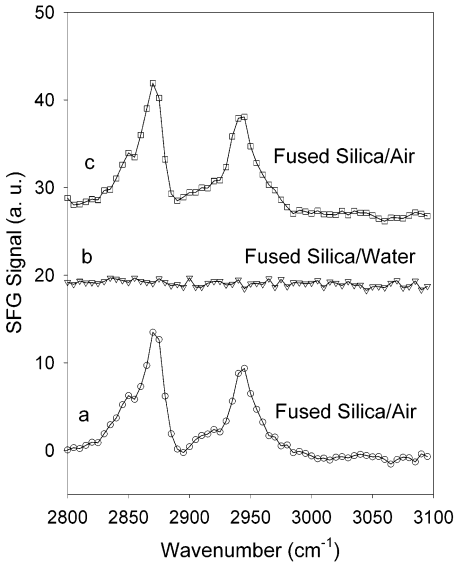

Figure 6. SFG spectra of fused silica (with adsorbed BSA)/air interface and fused silica (with adsorbed BSA)/water interface.

coverage of methyl groups on its surface in air.[23,26] The SFG signal intensity of the PBMA surface in air is only a few times stronger than that of the BSA solution in air. Similar analysis is applied to the peak around 3060 cm^{-1}, which is contributed by aromatic C−H stretches. The SFG signal from aromatic C−H is also quite strong compared to the relatively small amount of aromatic functional groups in BSA. These results indicate a strong alignment of the hydrophobic groups of the protein molecules at the interface.

We exclude the possibility that strong methyl and phenyl SFG signals are generated by the third-order nonlinear process caused by the electric field (i.e., by the net charges of adsorbed protein molecules)[51] because the SFG signal intensity of methyl groups has no noticeable change at pH $\sim$ 5 (not shown) where the electric field is much weaker. As proven above, the strong methyl and phenyl signals cannot be explained by the different Fresnal factors and local field correction factors across the protein film causing a signal despite the random orientation of BSA molecules (eq 6). Therefore, the only explanation to the strong methyl and phenyl SFG signals observed is that these groups have preferred orientations at the solution/air interface. By comparing the available data of BSA native structure, we believe that BSA molecules at the solution/air interface must undergo conformational changes. However, our SFG results indicate that these structures can generate similar C−H signals, showing that the alignment and order of C−H functional groups are still similar.

3.2.2. BSA Solution/Fused Silica Interface. SFG has been applied to investigate fused silica/BSA solution interfaces with BSA solutions of different pH. Different from BSA solution/air interfaces, SFG spectra only show the signals of O−H stretches of interfacial water molecules and no C−H signals of BSA molecules (Figure 5). These results are compatible with published results.[52] There are two possibilities for the absence of C−H signals from BSA solution/fused silica interfaces: (1) no BSA molecules can be adsorbed at fused silica/BSA solution interfaces and (2) all C−H groups such as methyl, methylene, and phenyl groups in the adsorbed BSA film have inversion symmetry, without net contribution to the SFG signal. Other techniques have been applied to examine BSA adsorption, indicating that BSA molecules can be adsorbed onto the fused silica surface.[53−57] Therefore, we believe that the absence of C−H signals in the SFG spectra collected from fused silica/BSA solution interfaces is due to the second possibility mentioned above. We have confirmed this by following experiments.

SFG spectra have been collected from the fused silica surface after it was removed from the BSA solution (with the pH value of $\sim$7), washed by water, and exposed to air. Strong C−H signals from BSA can be detected from this fused silica/air interface (Figure 6a). When we contacted this sample with water, the C−H signals disappeared (Figure 6b). After removing this sample from water again the SFG spectrum was collected; the spectrum was recovered. This clearly shows that BSA molecules were adsorbed on the fused silica/BSA solution interface. Because the refractive indices of fused silica, the adsorbed BSA layer, and the BSA solution are similar, the local optical field change across the BSA layer at the BSA solution/fused silica interface is small. Consequently, eqs 4 and 5 can be applied. The absence of the C−H signal is due to the fact that all C−H groups such as methyl, methylene, and phenyl groups in the adsorbed BSA film have inversion symmetry, without any net alignment along the surface normal. It is reasonable because the fused silica surface is very hydrophilic; therefore, when BSA molecules were adsorbed on the fused silica/BSA aqueous solution interface, the two sides of the absorbed protein layer are in contact with both hydrophilic environments. The hydrophobic components such as methyl and phenyl groups tend to bury inside the adsorbed layer then have no strong favorable orientation directing along the surface normal. Therefore, the adsorbed BSA has a "hydrophilic" conformation. The strong O−H signals are due to ordered interfacial water molecules orientated by the charged absorbed BSA layer.

We also confirmed our conclusion by removing the fused silica from the BSA solution and contacting it with hydrophobic solvents, including benzene, CCl_4, and FC-75 (a fluorinated hydrophobic solvent from 3M). The SFG spectra collected from silica/benzene, silica/CCl_4, and silica/FC-75 interfaces are shown in Figure 7. In Figure 7, C−H signals were visible and quite similar to each other. This is different from the fused silica−water situation. The FC-75 has a refractive index ($\sim$1.3) similar to water and different from benzene ($\sim$1.5) and CCl_4 ($\sim$1.46). The different SFG spectra at hydrophobic solvents and water interfaces are due to different orientation and/or conformation

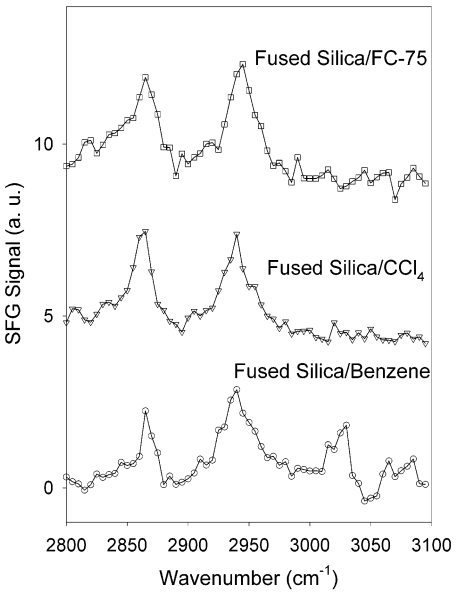

Figure 7. SFG spectra of fused silica (with adsorbed BSA)/benzene, fused silica (with adsorbed BSA)/CCl_4, fused silica (with adsorbed BSA)/FC-75 interfaces.

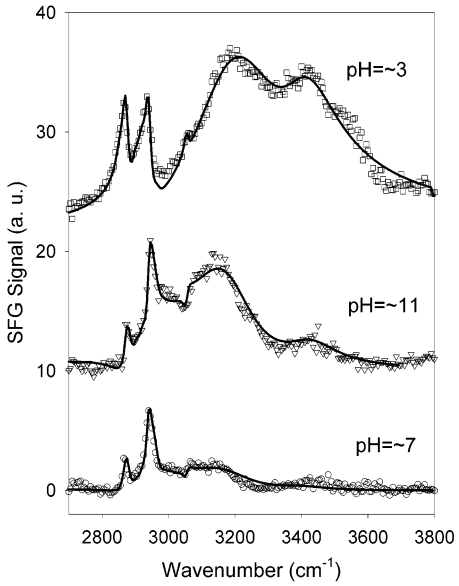

Figure 8. SFG spectra of d-PS/BSA solution interfaces with different solution pH values.

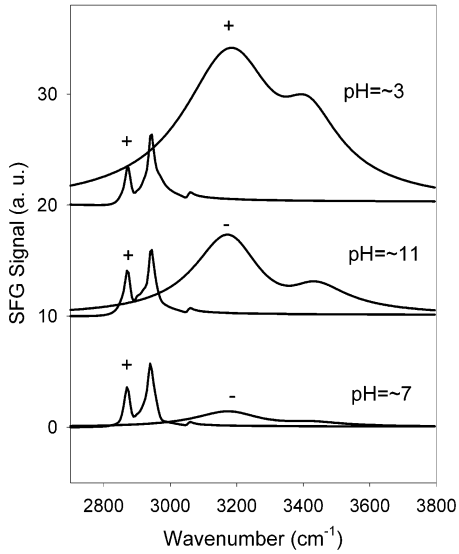

Figure 9. Fitting results for Figure 8.

of interfacial albumin molecules, rather than different local field effect of these interfaces. Otherwise, the SFG intensity should be very sensitive to the change of refractive indices. When these fused silica samples (with adsorbed BSA molecules) were removed from hydrophobic solvents and exposed to air, C−H signals were recovered.

When the fused silica surface was removed from the BSA solution, adsorbed BSA molecules stuck to the surface. Loosely deposited BSA molecules were washed off by water, but the strongly adsorbed BSA monolayer would still stay after the water wash. These BSA molecules presented at the fused silica and air interface mimicked the behavior of those at the solution/air interface; the hydrophobic components would align toward the air and their C−H signals would appear in the SFG spectra. The much stronger signal in air compared to contacting with hydrophobic solvents is an effect of Fresnel coefficient factor.

A fused silica prism has also been used to replace the fused silica window to study the fused silica/BSA solution interface. The SFG spectral intensity can be greatly enhanced by adopting this new experimental geometry. However, although the O−H signals have been enhanced, no C−H signals have been detected. It is clear that no C−H signals can be detected at the BSA solution/fused silica interface with different solution pH, indicating that BSA has "hydrophilic" conformations when adsorbed to fused silica at various solution pH.

3.2.3. BSA Solution/d-PS Interface. The SFG spectra of d-PS/BSA solution interfaces have been collected and shown in Figure 8. Unlike the spectra collected from fused silica/BSA solution interfaces, spectra displayed in Figure 8 show strong C−H signals. Figure 8 indicates that SFG spectra of d-PS/BSA solution with various pH are quite different. However, like the BSA solution/air interfaces, after fitting all of the spectra in Figure 8 quantitatively (fitting results are shown in Figure 9), it is clear that C−H signals are quite similar. Like the BSA solution/air interface, we found that the greatest factor affecting the spectra was the differences in phases of the O−H signals at different pH. As mentioned previously, this is a result of the water alignment at the charged protein layer.

For the BSA layer adsorbed at the BSA solution/d-PS interface, the Fresnal coefficient factors and local field factors across the layer are similar to the fused silica/BSA solution case. According to eqs 4 and 5, the different C−H signals at the interfaces involving d-PS and fused silica demonstrate that adsorbed BSA film has different structures at different interfaces. Unlike fused silica, the d-PS surface is hydrophobic. As with the BSA solution/air interface, at the d-PS/BSA solution interface, one side of the interfacial BSA molecules contacts the d-PS hydrophobic medium. Thus, BSA will not have a "hydrophilic"conformation; at the hydrophobic d-PS side, the hydrophobic components of BSA molecules would have preferential orientation; thus, SFG C−H signals can be detected.

Previous research of protein adsorption on different surfaces indicates that protein solution pH affects interfacial protein structures.[58−60] Our SFG C−H signals collected from BSA solution/air (and BSA solution/d-PS) interfaces show similar features for different BSA solution pH values. This indicates that these interfacial BSA molecules still have similar alignment and order of C−H functional groups. No C−H signals can be detected from BSA solution/fused silica interfaces, indicating that interfacial BSA molecules have hydrophilic conformations.

At different solution pH, these hydrophilic conformations may not be the same.

4. Conclusions

In this paper, we have studied BSA adsorbed on different contacting media at the contacting media/BSA solution interface using SFG. The SFG spectra collected from the BSA solution/air interfaces with different solution pH values are quite different, mainly because of the interferences between the C−H signals from interfacial BSA molecules and the O−H signals from water. The fitted spectra of C−H signals from BSA solution/air interfaces are similar at different solution pH. These results have been confirmed by SFG spectra collected from BSA D_2O solution/air interfaces. Similar results have been detected from BSA solution/d-PS interfaces with different solution pH. SFG spectra are different at different BSA solution interfaces, including the BSA solution/air, fused silica/BSA solution, and d-PS/BSA solution interfaces, indicating that structural changes of BSA molecules at different interfaces can be observed by SFG. No C−H signals of interfacial BSA molecules at the fused silica/BSA solution interfaces can be detected, showing that these absorbed BSA molecules have "hydrophilic" conformations. The conformation can be altered when adsorbed BSA on fused silica contacts different media, including air, water, and hydrophobic solvents. Our research on d-PS/BSA solution interface demonstrates that SFG can be applied to study protein adsorption on polymer materials in situ.

Acknowledgment. This research is supported by the Office of Naval Research (Grant No. N00014-02-1-0832), the start-up fund, and the 2002 Rackham Research Grant from the University of Michigan.

References and Notes

(1) Park, J. B.; Lakes, R. S. *Biomaterials: an Introduction*; Plenum Press: New York, 1992.
(2) Carbassi, F.; Morra, M.; Occhiello, E. *Polymer Surfaces: from Physics to Technology*; John Wiley and Sons: Chichester, U.K., 1994.
(3) Feast, W. J.; Munro, H. S.; Richards, R. W. *Polymer Surfaces and Interfaces II*; John Wiley and Sons: Chichester, U.K., 1987.
(4) Horbett, T. A.; Brash, J. L. *Proteins at Interfaces II, Fundamentals and Applications*; ACS Symposium Series 602; American Chemical Society: Washington, DC, 1995.
(5) Baier, R. E. *Applied Chemistry at Protein Interfaces*; American Chemical Society: Washington, DC, 1975.
(6) Brash, J. L., Horbett. T, A., Ed.; *Proteins at Interfaces, Physicochemical and Biochemical Studies*; American Chemical Society: Washington, DC, 1987.
(7) Ramsden, J. J. *Q. Rev. Biophys.* **1993**, *27*, 41.
(8) Woodruff, D.; Delchar, T. *Modern Techniques of Surface Science*; Cambridge University Press: Cambridge, U.K., 1986.
(9) Somorjai, G. A. *Introduction to Surface Chemistry and Catalysis*; Wiley: New York, 1994.
(10) Shen, Y. R. *The Principles of Nonlinear Optics*; Wiley: New York, 1984.
(11) Shen, Y. R. *Annu. Rev. Phys. Chem.* **1989**, *40*, 327.
(12) Miranda, P. B.; Shen, Y. R. *J. Phys. Chem. B* **1999**, *103*, 3292.
(13) Bain, C. D. *J. Chem. Soc., Faraday Trans.* **1995**, *91*, 1281.
(14) Eisenthal, K. B. *Chem. Rev.* **1996**, *96*, 1343.
(15) Walker, R. A.; Gruetzmacher, J. A.; Richmond, G. L. *J. Am. Chem. Soc.* **1998**, *120*, 6991.
(16) Gracias, D. H.; Chen, Z.; Shen, Y. R.; Somorjai, G. A. *Acc. Chem. Res.* **1999**, *320*, 930.
(17) Shultz, M. J.; Schnitzer, C.; Simonelli, D.; Baldelli, S. *Int. Rev. Phys. Chem.* **2000**, *19*, 123.
(18) Pizzolatto, R. L.; Yang, Y. J.; Wolf, L. K.; Messmer, M. C. *Anal. Chim. Acta* **1999**, *397*, 81.
(19) Kim, J.; Cremer, P. S. *J. Am. Chem. Soc.* **2000**, *122*, 12371.
(20) Briggman, K. A.; Stephenson, J. C.; Wallace, W. E.; Richter, L. J. *J. Phys. Chem. B* **2001**, *105*, 2785.
(21) Gautam, K. S.; Schwab, A. D.; Dhinojwala, A.; Zhang, D.; Dougai, S. M.; Yeganeh, M. S. *Phys. Rev. Lett.* **2000**, *85*, 3854.
(22) Löbau, J.; Wolfrum, K. *J. Opt. Soc. Am. B* **1997**, *14*, 2505.
(23) Wang, J.; Woodcock, S. E.; Buck, S. M.; Chen, C. Y.; Chen, Z. *J. Am. Chem. Soc.* **2001**, *123*, 9470.
(24) Wang, J.; Chen, C. Y.; Buck, S. M.; Chen, Z. *J. Phys. Chem. B* **2001**, *105*, 12118.
(25) Chen, C.; Wang, J.; Woodcock, S. E.; Chen, Z. *Langmuir* **2002**, *18*, 1302.
(26) Wang, J.; Paszti, Z.; Even, M. A.; Chen, Z. *J. Am. Chem. Soc.* **2002**, *124*, 7016.
(27) Wilk, D.; Johannsmann, D.; Stanners, C.; Shen, Y. R. *Phys. Rev. B* **1995**, *51*, 10057.
(28) Guyot-Sionnest, P.; Chen, W.; Shen, Y. R. *Phys. Rev. B* **1986**, *33*, 8254.
(29) Guyot-Sionnest, P.; Shen, Y. R. *Phys. Rev. B* **1987**, *35*, 4420.
(30) Ye, P.; Shen, Y. R. *Phys. Rev. B* **1983**, *28*, 4288.
(31) Zyss, J.; Oudar, J. L. *Phys. Rev. A* **1982**, *26*, 2028.
(32) Oudar, J. L.; Zyss, J. *Phys. Rev. A* **1982**, *26*, 2016.
(33) Hirose, C.; Akamtsu, N.; Domen, K. *Appl. Spectrosc.* **1992**, *46*, 1051.
(34) Jackson, J. D. *Classical Electrodynamics*, 2nd ed.; Wiley: New York, 1975.
(35) Zhuang, X.; Miranda, P. B.; Kim, D.; Shen, Y. R. *Phys. Rev. B* **1999**, *59*, 12632.
(36) Lu, J. R.; Su, T. J.; Penfold, J. *Langmuir* **1999**, *15*, 6975.
(37) Tripp, B. C.; Magda, J. J.; Andrade, J. D. *J. Colloid Interface Sci.* **1995**, *173*, 16.
(38) Miller, R.; Fainerman, V. B.; Makievski, A. V.; Krägel, J.; Grigoriev, D. O.; Kazakov, V. N.; Sinyachenko, O. V. *Adv. Colloid Interface Sci.* **2000**, *86*, 39.
(39) Wen, X.; Franses, E. I. *Colloid Surf. A* **2001**, *190*, 319.
(40) Murray, B. S. *Colloid. Surf. A* **1997**, *125*, 73.
(41) Ybert, C.; di Meglio, J. M. *Langmuir* **1998**, *14*, 471.
(42) Rosenoer, V. M., Oratz, M., Rothschild, M. A., Ed.; *Albumin Structure, Function and Uses*; Pergamon: Oxford, 1977.
(43) Peters, T. *Adv. Protein Chem.* **1985**, *37*, 161.
(44) Bendedouch, D.; Chen, S. H. *J. Phys. Chem.* **1983**, *87*, 1473.
(45) He, X. M.; Carter, D. C. *Nature* **1992**, *358*, 209.
(46) Carter, D. C.; Ho, J. X. *Adv. Protein Chem.* **1994**, *45*, 153.
(47) Sadler, P. J.; Tucker, A. *Eur. J. Biochem.* **1992**, *205*, 631.
(48) Wei, X.; Hong, S. C.; Zhuang, X. W.; Goto, T.; Shen, Y. R. *Phys. Rev. E* **2000**, *62*, 5160.
(49) Oh-e, M.; Lvovsky, A. I.; Wei, X.; Shen, Y. R. *J. Chem. Phys.* **2000**, *113*, 8827.
(50) Hirayama, K.; Akashi, S.; Furuya, M.; Fukuhara, K. I. *Biochem. Biophys. Res. Commun.* **1990**, *173*, 639.
(51) Gragson, D. E.; Richmond, G. L. *J. Phys. Chem. B* **1998**, *102*, 3847.
(52) Kim, J.; Cremer, P. S. *ChemPhysChem* **2001**, *8/9*, 543.
(53) Kurvat, R.; Prenosil, J. E.; Ramsden, J. J. *J. Colloid Interface Sci.* **1997**, *185*, 1.
(54) Su, T. J.; Lu, J. R.; Thomas, R. K.; Cui, Z. F.; Penfold, J. *J. Phys. Chem. B* **1998**, *102*, 8100.
(55) Giacomelli, C. E.; Norde, W. *J. Colloid Interface Sci.* **2001**, *233*, 234.
(56) Norde, W.; Giacomelli, C. E. *J. Biotechnol.* **2000**, *79*, 259.
(57) Norde, W.; Anusiem, A. C. I. *Colloid. Surface.* **1992**, *66*, 73.
(58) Servagent-Noinville, S.; Revault, M.; Quiquampoix, H.; Baron, M. H. *J. Colloid Interface Sci.* **2000**, 221, 273.
(59) Norde, W.; Favier, J. P. *Colloid Surf.* **1992**, *64*, 87.
(60) Kim, G.; Gurau, M.; Kim, J.; Cremer, P. S. *Langmuir* **2002**, *18*, 2807.